
Uniaxial/Biaxial Stress Paradox in Optical-Materials Hardening

Owing to its excellent homogeneity and low-intrinsic absorption properties, fused silica remains the preferred material for high-power laser applications over a wide wavelength range, but especially in the UV. In particular, large-aperture glass and excimer lasers, such as Nova, Beamlet, OMEGA, NIKE, and, in the foreseeable future, the National Ignition Facility (NIF), the Megajoule laser (LMJ, France), and others, owe their existence to readily available, large-diameter fused silica finding use in the form of beam-transport lenses and windows. Often these lenses and windows separate atmospheric pressure from vacuum areas, such as on spatial filters and target tanks, experiencing not only high-fluence irradiation conditions but also pressure-differential-induced stresses. The combination of the two presents an interesting challenge in terms of laser damage, as the formation of pits and cracks during conventional damage may get aggravated by the presence of stress and lead to dramatic device failure by fragmentation and acceleration of the lens or window shards into the evacuated space.

Even in the absence of a vacuum issue with its concomitant stress, laser damage to fused silica under periodic illumination by UV light, such as found in UV-lithography or medical-instrument applications, limits system performance and increases maintenance costs. This motivates the search for simple methods to alleviate the onset of or, at least, the detrimental consequences of laser damage. In earlier work,¹⁻⁴ dynamic aspects of laser-induced crack formation in fused silica and its correlation with stress, both self-induced² and externally applied,^{3,4} have been studied by us with an eye toward preparing the foundation for such remedies. In the current work, we try to answer several important questions raised by this prior work.

In brief, a laser-initiated crack has been shown to grow upon repeated irradiation by either IR⁵ or UV^{1,5} laser pulses, causing a *hoop stress*² to form in its immediate surroundings, the existence of which is essential for further growth. This causal relation was tested by breaking the *hoop-stress symmetry* with the help of an external stress field and thereby arresting further crack propagation, even at pump fluences much larger than

those necessary for starting the crack initially. This was demonstrated for fused silica initiated at either the substrate exit or entrance surface. Surfaces, with few exceptions, suffer from lower laser-damage thresholds than bulk—a fact attributable to the consequences of the requisite, but extremely intrusive, acts of cutting, grinding, polishing, and cleaning the surfaces. Cleaved surfaces that are spared these procedures offer comparably higher damage thresholds.⁶ The surfaces of fused silica are of special interest in that a *near-surface layer* of material *densification*⁷ is surmised to be formed during polishing, which, by itself, may prompt *near-surface residual-stress fields* to develop. One key question arising from the prior work^{3,4} thus became whether or not, in the absence of a densification layer and its residual-stress field, the effects observed in fused silica will remain. Or, put another way, will externally applied stresses also delay laser-damage initiation in cleaved silica bulk and/or in materials for which no such densification layer exists? To find the answer, this work addresses, in addition to polished fused silica, alternate model systems: cleaved silica bulk and BK-7, borosilicate glass.

A second question arises from the earlier *observed increase in surface-damage initiation threshold and crack growth arrest* with external stresses applied in the laser-beam direction. The question is whether or not the direction of the applied load has an effect on the surface-damage initiation threshold and crack growth. To answer this question, different applied load configurations are considered in this work; among them are the uniaxial compressions in the x or z direction, the biaxial compression in the x and z directions for rectangular samples (fused silica and BK-7), as well as radially applied pressure for round fused-silica samples.

Sample irradiation was carried out by the fundamental and frequency-tripled outputs of a Nd:glass oscillator/single-pass amplifier system. This system produced a beam of nearly Gaussian profile after passage through a vacuum spatial filter, prior to any frequency conversion. The beam was then focused by a 2-m-focal-length fused-silica lens to a $\sim 600\text{-}\mu\text{m}$ spot size

at the sample entrance surface. Laser pulses, produced at a repetition rate of one pulse every 10 s, had nominal pulse duration of 1 ns at 1053 nm and 500 ps at 351 nm.

A PDP-II computer and CAMAC [computer-aided measurement and control (J. White Co. 800)] crate system were used for data acquisition and experiment control. The system included a charge-injection-device (CID) camera located in a sample-equivalent plane for recording the fluence distribution in the beam spot.

The beam-incident direction was chosen to be $\leq 10^\circ$ off-normal to the sample entrance face to prevent any back-reflection of residual, unconverted IR from seeding the amplifier in the backward direction, and setting up a 351-nm Fresnel interference pattern between the sample entrance and exit surfaces that would invalidate the calculated fluence distribution.

In this work, *damage* is defined to be any visible permanent modification to the surface of the glass material, observable with a 110 \times -magnification, dark-field microscope. The smallest damage spots observed as faint scatter sites were approximately 0.5 to 1 μm in diameter. Due to the thickness of the samples, spatial and temporal distortions of the beam were avoided; therefore, both front- and exit-surface damages were considered. Damage thresholds were determined by averaging between the highest laser fluence incident on the sample that produced no damage and the lowest laser fluence that did produce damage.

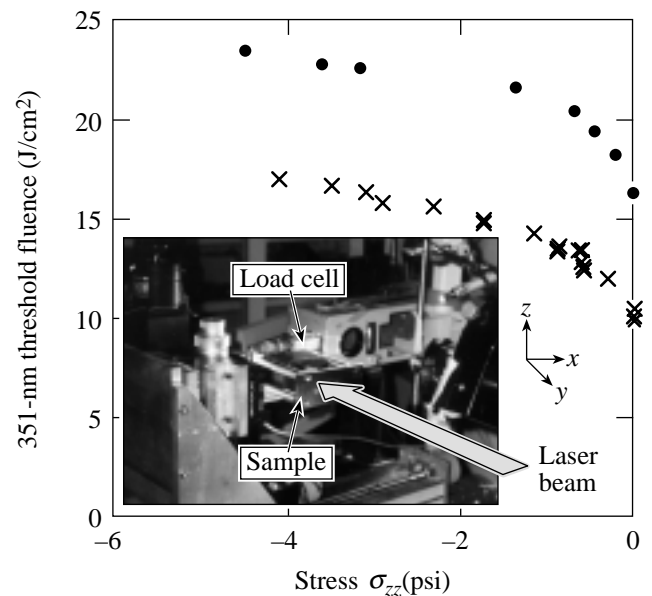
The samples studied in this work were rectangular, 64 \times 13.6 \times 4.3-mm and circular, 50-mm-diam, fused-silica samples of Corning 7940 UV, grade A. They were conventionally pitch polished to *laser quality* (rms $\leq 10 \text{ \AA}$) on the entrance and exit surfaces and to *cosmetic quality* around the edges to monitor *in situ* the crack propagation, as were the BK-7 samples, which were also commercial blocks (52 \times 11.5 \times 5 mm).

Samples were mechanically loaded by clamping each between aluminum plates separately attached to a load cell (Eaton, Model 3397-25, max. load capacity: 25 lbs). A predetermined, constant uniaxial, compressive load was applied in each geometrical configuration. Details of the experimental setup of the applied load used in the laser-beam direction can be found in Ref. 8.

Laser-damage thresholds (for pulse lengths greater than picoseconds) are always reported as *average values* derived

from a statistical number of sample sites *per tested specimen*. In all *nondeterministic*, i.e., extrinsic-impurity-driven laser-damage processes, the damage occurrence hinges on the statistical presence or absence of one or more absorbing impurities within a given irradiated area. This statistical distribution in defect volume density is now convoluted by a site-to-site-varying stress distribution. In an ideal experiment, a large enough number of tests on samples and sites with precisely known local stress will deconvolve the two distributions. In practice, however, this is unrealistic. Rather, simulation of local stress conditions by finite-element methods permits one to find with acceptable accuracy, for various loading-geometry-boundary conditions, the stresses within the aperture, based on which one may choose many irradiation sites on a single sample. A three-dimensional, finite-element analysis code ANSYS 5.4A[®], developed by ANSYS Inc., was used to determine the stress distribution within loaded samples.

Figure 79.62 shows the 500-ps/351-nm damage-onset fluence threshold for fused-silica exit and entrance surfaces versus the stress σ_{zz} resulting from a compressive load in the laser-beam direction. The question to address is whether or not a link exists between the silica surface-densification layer (and its residual-stress distribution) and the damage-threshold



G4786

Figure 79.62

Entrance (●)- and exit (×)-surface, 351-nm damage-initiation thresholds as functions of applied stress in fused silica for the laser beam direction-loading configuration.

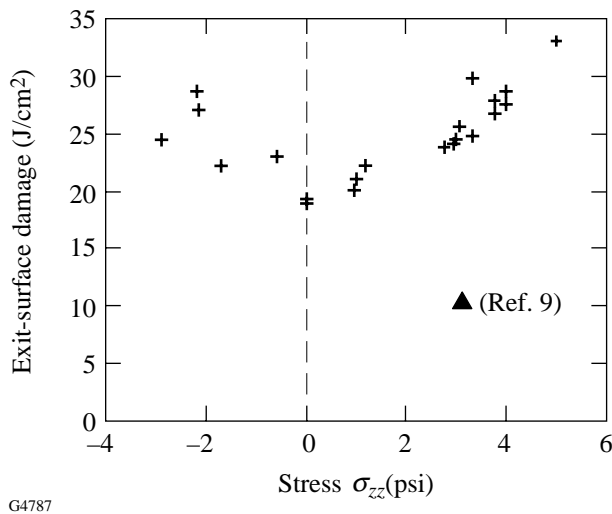
trend. Applying external stresses will bias these effects. In light of Fig. 79.62, it appears plausible that increasing stresses within the sample are decreasing the effect of the densified layer and, at the same time, are increasing the damage-onset threshold. To confirm or rule out this premise, further tests were needed on cleaved silica bulk and on a material that does not densify when polished. Figure 79.63 displays the exit-surface-damage-threshold results versus applied stress obtained for BK-7 with 1-ns, 1053-nm pulses. A data point from Ref. 9, obtained at 1 ns, 1064 nm (also represented in Fig. 79.63), shows good agreement with our *stress-free* measurements. Furthermore, Fig. 79.64 illustrates the front-surface-damage thresholds against the externally applied stresses obtained for cleaved bulk silica. From Figs. 79.63 and 79.64, it becomes clear that a damage-initiation-threshold enhancement in response to externally applied stress is also obtained for borosilicate glass as well as for cleaved bulk silica, ruling out causal relations between densification, applied stress, and damage-initiation-threshold enhancement in all systems considered here.

Next, we address correlations between (1) the external stress and the laser-beam polarization and/or (2) the external stress and thermal stress. In other words, (1) What is the effect of external stress on the damage threshold and crack growth for a certain beam polarization? and (2) What is the magnitude of transient, thermal stresses induced by laser heating of

the material compared to the magnitude of the externally applied stresses?

The answer to the second question was obtained by using ANSYS in a thermal, transient analysis. A metallic defect (Hf) of size $200 \times 200 \times 100 \text{ \AA}$ embedded in the fused-silica matrix was considered and assumed to have reached a temperature of 20,000 K by the end of the laser pulse (1 ns). Details of the transient thermal finite-element analysis can be found in Ref. 10. The thermal stresses deduced from ANSYS $\{-\alpha E \Delta T$, where α is the thermal expansion coefficient, E the Young's modulus, and ΔT the temperature [relative to the strain-free temperature (room temperature)] of a given point in the matrix} were found to be two orders of magnitude larger than the applied mechanical stresses, rendering them all but irrelevant.

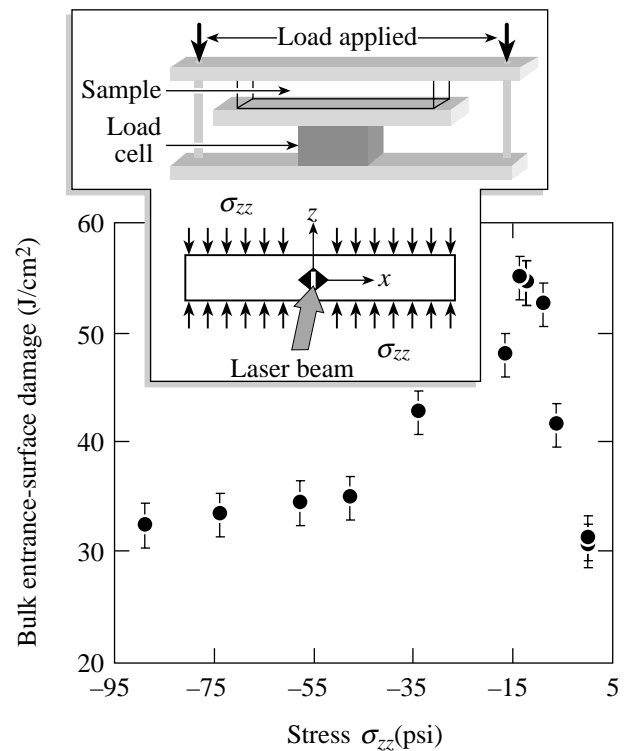
The issue of mechanical stress versus beam polarization was addressed by using the original loading setup in two different geometrical loading configurations; the load was first applied in the x direction (Fig. 79.65), and second in the z direction (Fig. 79.66). For these two configurations, the result-



G4787

Figure 79.63

Exit-surface, 1053-nm damage-initiation threshold as a function of externally applied stresses obtained with borosilicate glass (BK-7) for the same loading configuration as Fig. 79.62. For comparison a data point (triangle) obtained at 1064 nm, 1 ns from Ref. 9 is reported.



G4788

Figure 79.64

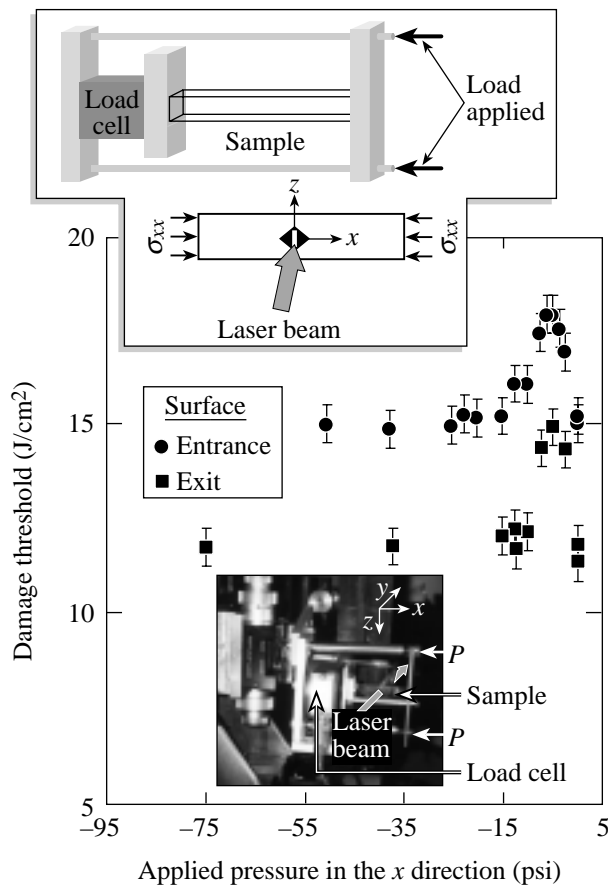
Entrance-surface, 351-nm, 500-ps, damage-initiation threshold as functions of applied pressure in the z direction (perpendicular to the laser beam) in cleaved silica bulk.

ing stress estimated from ANSYS is uniaxial along the x axis or the z axis, respectively. For uniaxial stress, Figs. 79.65 and 79.66 show the damage threshold to reach a maximum around -5 psi and to drop to its initial, stress-free value for loads larger than -15 psi. The same behavior was obtained with BK-7 loaded in the z direction (Fig. 79.66), ruling out any relationship between the stress-onset damage threshold and the laser-beam polarization.

To investigate the effect of the loading geometry on the damage threshold, a setup was designed that provided simultaneous stresses in both the x and z directions. Figure 79.67 shows the results obtained with this configuration for both entrance and exit surfaces of fused silica. The damage threshold reaches a maximum around $\sigma_{zz} = \sigma_{xx} = -5$ psi and stays constant thereafter, a behavior similar to that found for the

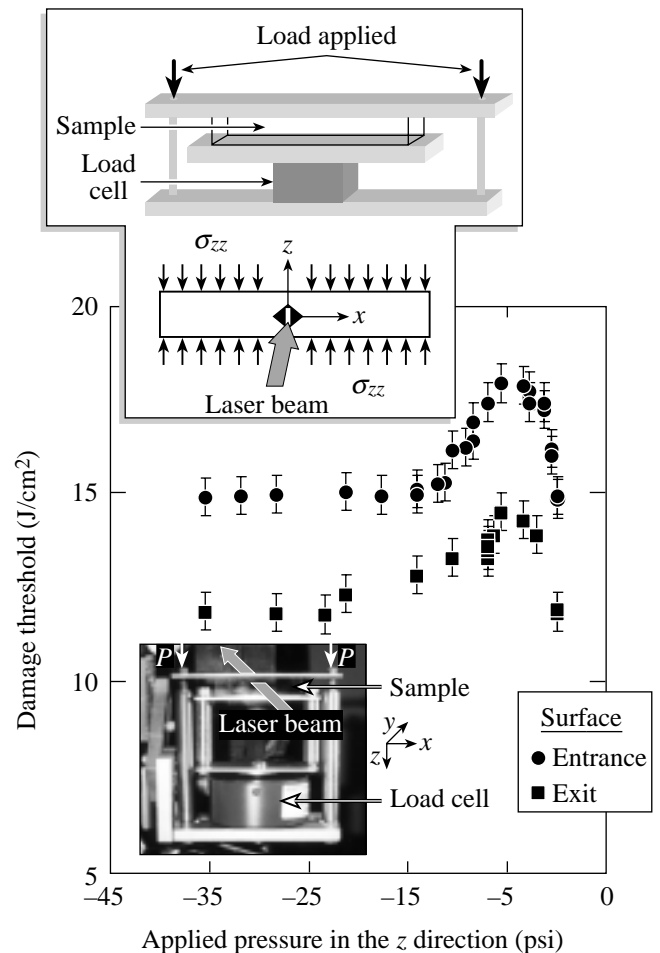
configuration in Fig. 79.62, where the ANSYS-derived stress distribution shows stresses in both the x and z directions, although $\sigma_{zz} > \sigma_{xx}$. On the other hand, experiments carried out on circular fused-silica samples are illustrated in Fig. 79.68. Although the current setup did not permit pressures larger than 4.2 psi to be applied, Fig. 79.68 hints that the maximum threshold would be reached also around 4 to 5 psi.

Key results from Fig. 79.62 and Figs. 79.65–79.68 are: (1) Independently of the loading geometry used, the maximum threshold for fused silica is obtained around an applied stress of -5 psi. (2) A geometrical loading approximating practical situations is that of Fig. 79.62, where a plateau is reached (the configuration used in Fig. 79.67 is very difficult to implement in practice).



G4789

Figure 79.65 Entrance- and exit-surface, 351-nm, 500-ps damage-initiation thresholds as functions of applied pressure in the x direction (perpendicular to the laser beam) in polished fused silica. The load P is applied via two screws.



G4790

Figure 79.66 Entrance- and exit-surface, 351-nm, 500-ps damage-initiation thresholds as functions of applied pressure in the z direction (perpendicular to the laser beam) in polished fused silica. The load P is applied via two screws.

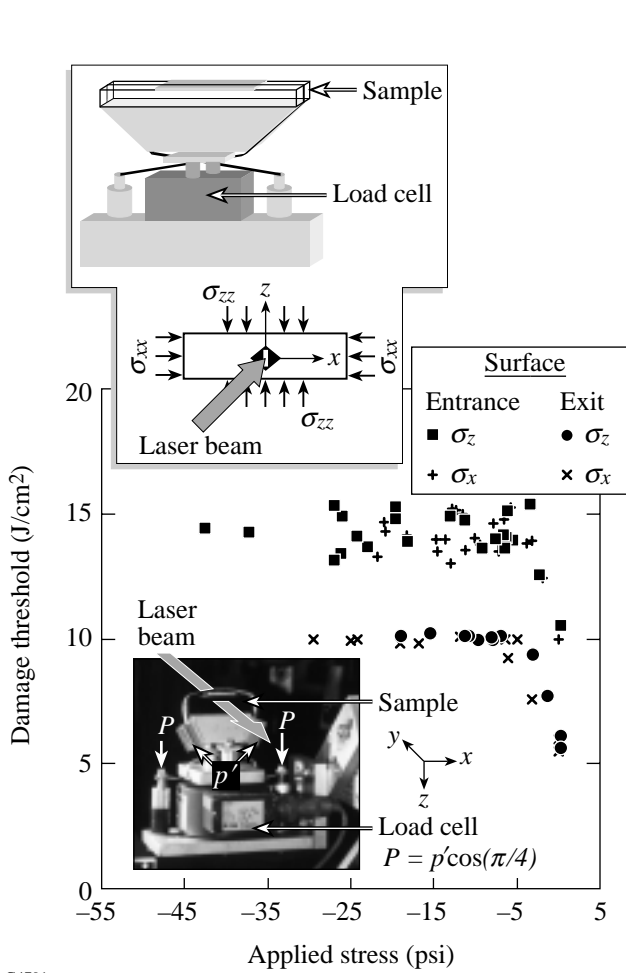
Experiments on crack growth using *uniaxial* stress configurations were also carried out, but *no crack arrest* was observed for any of these configurations, leading one to conclude again that the optimum result for both damage-threshold enhancement and crack-growth arrest in fused silica can be obtained only in a biaxial stress configuration.

In conclusion, this work presents experimental results on stress-inhibited, laser-driven crack growth and stress-delayed, laser-damage-initiation thresholds in fused silica and borosilicate glass (BK-7). The use of different loading geometries providing uniaxial and biaxial stresses shows that the *biaxial* stress configuration offers superior efficiency in raising the

laser-damage-initiation threshold by up to 78% and arresting crack growth down to 30% relative to stress-free conditions. The results also raise the intriguing paradox of biaxial symmetry breaking proving superior to uniaxial effects—a paradox that calls for further tests.

ACKNOWLEDGMENT

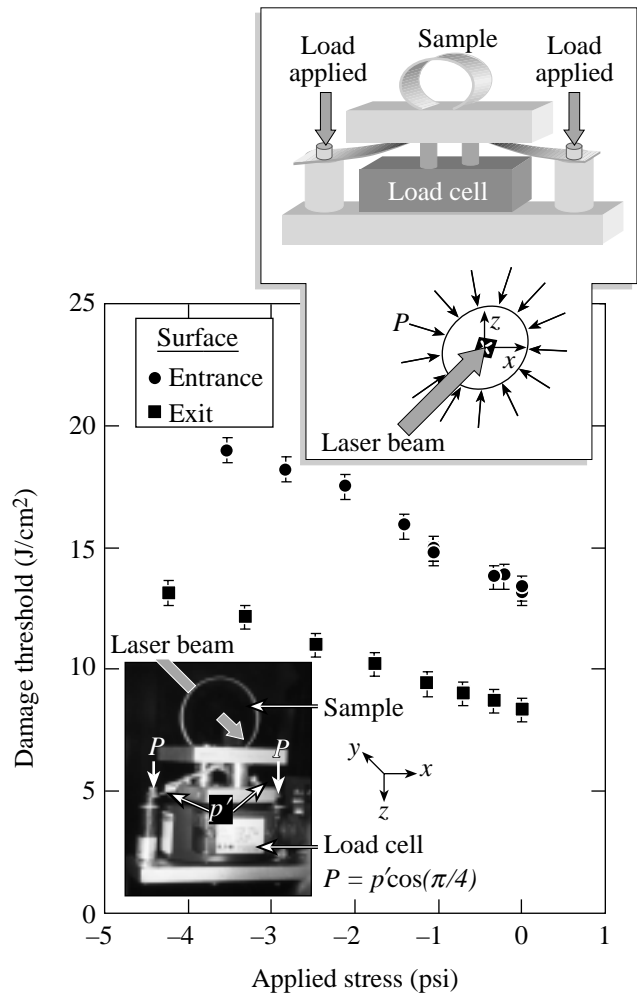
This work was supported by the U.S. Department of Energy Office of Inertial Confinement Fusion under Cooperative Agreement No. DE-FC03-92SF19460, the University of Rochester, and the New York State Energy Research and Development Authority. The support of DOE does not constitute an endorsement by DOE of the views expressed in this article.



G4791

Figure 79.67

Entrance- and exit-surface, 351-nm, 500-ps damage-initiation thresholds as functions of applied stresses in polished fused silica for the case of a compression load in the *x-z* plane.



G4792

Figure 79.68

Entrance- and exit-surface, 351-nm, 500-ps damage-initiation thresholds as functions of applied pressure in round, polished-fused-silica samples.

REFERENCES

1. F. Dahmani, J. C. Lambropoulos, A. W. Schmid, S. Papernov, and S. J. Burns, *J. Mater. Res.* **14**, 597 (1999).
2. F. Dahmani, A. W. Schmid, J. C. Lambropoulos, and S. Burns, *Appl. Opt.* **37**, 7772 (1998).
3. F. Dahmani, S. J. Burns, J. C. Lambropoulos, S. Papernov, and A. W. Schmid, *Opt. Lett.* **24**, 516 (1999).
4. F. Dahmani, J. C. Lambropoulos, A. W. Schmid, S. Papernov, and S. J. Burns, "Crack Arrest and Stress Dependence of Laser-Induced Surface Damage in Fused Silica and Borosilicate Glass," submitted to *Applied Optics*.
5. A. Salleo, R. Chinsio, and F. Y. Génin, in *Laser-Induced Damage in Optical Materials: 1998*, edited by G. J. Exarhos *et al.* (SPIE, Bellingham, WA, 1998), Vol. 3578, pp. 456–471.
6. S. Papernov, D. Zaksas, J. F. Anzellotti, D. J. Smith, A. W. Schmid, D. R. Collier, and F. A. Carbone, in *Laser-Induced Damage in Optical Materials: 1997*, edited by G. J. Exarhos *et al.* (SPIE, Bellingham, WA, 1998), Vol. 3244, pp. 434–445.
7. H. Yokota *et al.*, *Surf. Sci.* **16**, 265 (1969).
8. Laboratory for Laser Energetics LLE Review **77**, 26, NTIS document No. DOE/SF/19460-284 (1998). Copies may be obtained from the National Technical Information Service, Springfield, VA 22161.
9. F. Rainer, R. P. Gonzales, and A. J. Morgan, in *Laser-Induced Damage in Optical Materials: 1989*, Natl. Inst. Stand. Technol. (U.S.), Spec. Publ. 801 (U.S. Government Printing Office, Washington, DC, 1990), Vol. 1438, pp. 58–73.
10. S. Papernov and A. W. Schmid, *J. Appl. Phys.* **82**, 5422 (1997).

